Murti, V. V. S., Seshadri, T. R., and Venkitasubramanian, T. A. (1964), *Phytochemistry 3*, 73.
Newton, W. A., and Snell, E. E. (1964), *Proc. Nat. Acad. Sci. U. S. 51*, 382.
Pollara, B., and Von Korff, R. W. (1960), *Biochim. Biophys. Acta 39*, 364.
Rabinowitz, M., Olson, M. E., and Greenberg, D. M. (1954), *J. Biol. Chem. 210*, 837.
Rao, S. L. N., Adiga, P. R., and Sarma, P. S. (1964), *Biochemistry 3*, 432.
Rao, S. L. N., Malathi, K., and Sarma, P. S. (1969), *World Rev. Nutr. Diet. 10*, 214.
Rao, S. L. N., and Sarma, P. S. (1967), *Biochem. Pharmacol. 16*, 220.
Rao, S. L. N., Sarma, P. S., Mani, L. S., Rao, T. R. R., and Sriramachari, S. (1967), *Nature (London) 214*, 610.
Reid, K. G., Utech, N. M., and Holden, J. T. (1970), *J. Biol. Chem. 245*, 5261.
Robbins, J. (1959), *J. Physiol. (London) 148*, 39.
Rosen, H. (1957), *Arch. Biochem. Biophys. 67*, 10.
Roy, D. N., Nagarajan, V., and Gopalan, C. (1963), *Cur. Sci. 32*, 116.
Roy, D. N., and Rao, B. S. N. (1968), *Curr. Sci. 37*, 395.
Russell, D. W. (1963), *Biochem. J. 87*, 1.
Sanger, F. (1945), *Biochem. J. 39*, 507.
Sarma, P. S., and Padmanaban, G. (1969), *in* Toxic Constituents of Plant Foodstuffs, Liener, I. E., Ed., New York, N. Y., Academic Press, p 267.
Schneider, F. (1937), *Justus Liebigs Ann. Chem. 529*, 1.
Shearn, A., and Horowitz, N. H. (1969), *Biochemistry 8*, 295.
Surdin, Y., Sly, W., Sire, J., Bordes, A. M., and De Robichon-Szulmajster, H. (1965), *Biochim. Biophys. Acta 107*, 546.
Takeuchi, A., and Takeuchi, N. (1964), *J. Physiol. (London) 170*, 296.
Takeuchi, A., and Takeuchi, N. (1965), *J. Physiol. (London) 177*, 225.
Usherwood, P. N. R., Machili, P., and Leaf, G. (1968), *Nature (London) 219*, 1169.
Van Harreveld, A., and Mendelson, M. (1959), *J. Cell. Comp. Physiol. 54*, 85.
Watkins, J. C., Curtis, D. R., and Biscoe, T. J. (1966), *Nature (London) 211*, 637.
Wickerham, L. J. (1951), *U. S. Dep. Agr. Tech. Bull. 1029*, 7.
Wilds, A. L., and Shunk, C. H. (1948), *J. Amer. Chem. Soc. 70*, 2427.
Wofsey, A. R., Kuhar, M. J., and Snyder, S. H. (1971), *Proc. Nat. Acad. Sci. U. S. 68*, 1102.

Molecular Composition and Sedimentation Characteristics of Soluble Antigen–Antibody Complexes†

William P. Arend,* David C. Teller, and Mart Mannik

ABSTRACT: Soluble antigen(Ag)–antibody(Ab) complexes are formed in the presence of excess antigen. A limiting small immune complex is formed in high degrees of antigen excess. The molecular compositions of human serum albumin–anti-human serum albumin (rabbit) and bovine serum albumin–anti-bovine serum albumin (rhesus) complexes were investigated by ultracentrifugation. The two major species of limiting complexes were 11.0 S and 8.5 S, as determined by zonal ultracentrifugation, and 11.7 S and 9.0 S by analytical ultracentrifugation, with the smaller complexes predominating in moderate degrees of antigen excess. The molar composition of these complexes was determined by zonal ultracentrifugation using ^{131}I- and ^{125}I-labeled antigens and antibodies, respectively. The molar composition of the 11.0S complexes was Ag_2Ab_2 and the smaller complexes consisted of primarily Ag_1Ab_1. A computer model of the smaller complexes was constructed using current hydrodynamic and electron microscopic data for γG and bovine serum albumin molecules. Calculations of theoretical sedimentation coefficients disclosed that Ag_2Ab_1 and Ag_1Ab_1 complexes cannot be separated adequately by analytical ultracentrifugation, and that the Ag_1Ab_1 complexes observed experimentally did not result from dissociation of larger complexes. Thus the smallest, or limiting complex, in low to moderate degrees of antigen excess is predominantly Ag_1Ab_1.

Molecules of the γG[1] class of antibodies are bivalent. Antigens, however, may be monovalent to multivalent. Multivalent antigens form precipitates with their specific antibodies in the zone of antibody excess as well as at antigen–antibody equivalence due to lattice formation. Further increase in the amount of antigen results in a decrease of the precipitate and the formation of soluble antigen–antibody complexes. Complexes formed at low degrees of antigen excess are larger, with more lattice work, and possess more

† From the Department of Medicine, Veterans Administration Hospital, Seattle, Washington 98108, and the Division of Rheumatology, Department of Medicine, and the Department of Biochemistry, University of Washington School of Medicine, Seattle, Washington 98195. *Received April 5, 1972.* This work was supported in part by Research Grant AM11476 and Training Grant AM5602, both from the National Institute of Arthritis and Metabolic Diseases, and by GM13401 from the National Institute of General Medical Sciences.

* Author to whom correspondence should be addressed at the University of Washington School of Medicine, Division of Rheumatology. Recipient of a Research and Education Associateship from the Veterans Administration.

[1] Abbreviations used are: Ag, antigen; Ab, antibody; HSA, human serum albumin; BSA, bovine serum albumin; γG, γG-globulin; anti-HSA or anti-BSA, antibodies directed against HSA or BSA.

biological properties than complexes formed at higher degrees of antigen excess (Ishizaka, 1963; Mannik *et al.*, 1971). As the degree of antigen excess is increased, the complexes approach a minimal size, called the limiting complex. The molar ratio of the limiting complex with multivalent antigens has been concluded to be Ag_2Ag_1 by many workers (Singer and Campbell, 1952; Weigle and Maurer, 1957; Mulligan *et al.*, 1966). This molecular ratio was felt to be thermodynamically the most stable in comparison with the other possible configurations, *e.g.*, Ag_1Ab_1, Ag_1Ab_2, and Ag_2Ab_2.

Recent studies (Mannik *et al.*, 1971; Arend and Mannik, 1971; Mannik and Arend, 1971) indicated that some biological properties of soluble immune complexes, including clearance from rabbit circulation, and complement fixation, were related to the molecular composition of the complexes in that it was necessary for more than two antibody molecules to be present before the complexes acquired these biological activities. The conclusion was reached that the molar ratio of the limiting complex in antigen excess was not necessarily Ag_2Ab_1.

The present studies were designed to determine the sedimentation coefficients of soluble complexes by analytical ultracentrifugation, and to determine the molar Ag/Ab ratios of the complexes. In addition, theoretical sedimentation coefficients were calculated by a computer model of soluble antigen–antibody complexes of varying configurations. Two separate antigen–antibody systems were studied: HSA–anti-HSA (rabbit antibodies), and BSA–anti-BSA (rhesus monkey antibodies). The data supported the conclusion that in both systems the limiting complexes in low to moderate degrees of antigen excess were Ag_2Ab_2 and Ag_1Ab_1.

Materials and Methods

Preparation of Antigens and Antibodies. The details of preparative procedures have been presented (Mannik *et al.*, 1971), therefore, only a summary is included here. New Zealand rabbits were hyperimmunized with HSA in complete Freund's adjuvant. Thereafter they were bled at weekly intervals. For some studies, rabbits were immunized intravenously with 10 mg of HSA in normal saline, and boosted at 10 days with 20 mg of HSA in saline injected intraperitoneally. These rabbits were bled at 15 and 17 days and exsanguinated at 20 days after the initial intravenous immunization. Approximately 5-kg rhesus monkeys (*Macaca mulatta*) were hyperimmunized with BSA in complete Freund's adjuvant , with an immunization and bleeding schedule similar to that utilized for the rabbits. All antisera were stored at −20° until further purification of antibodies was carried out.

Antibodies were isolated by solid-phase immunoadsorbents, utilizing antigen–agarose columns (Mannik and Stage, 1971). Specific antibodies were adsorbed from the antisera, and the columns were exhaustively washed with sodium borate buffer (0.2 M borate–0.16 M NaCl, pH 8.0). The antibodies were eluted from the immunoadsorbent columns with 0.01 M HCl–0.15 M NaCl (pH 2.0) or with unbuffered (neutral pH) 2.5 M KI, and then dialyzed against large volumes of borate buffer. Antibodies and antigens were trace labeled with ^{125}I or ^{131}I, respectively, by the iodine monochloride method (Helmkamp *et al.*, 1960), yielding 1–2 moles of iodine per mole of protein. Free isotope was removed by exhaustive dialysis against borate buffer. All antigen and antibody preparations were made aggregate free by gel filtration on Sephadex G-200 after labeling, and the monomeric γG or albumin solutions were utilized for studies within a few weeks. In all preparations more than 98% of the proteins were in monomeric form, as determined by sucrose density gradient ultracentrifugation, and greater than 99% of the radioactivity was protein bound.

Preparation of Immune Complexes. Precipitin curves were constructed for each antigen–antibody system, and the point of equivalence was determined. At equivalence, 85–90% of the rabbit antibodies against HSA precipitated, and 45% of the rhesus antibodies against BSA were precipitated. The reasons for incomplete precipitation of isolated antibodies were not elucidated, but three possibilities existed: some antibodies may have been denatured by elution procedures, possibly some antibodies were nonprecipitating, or normal γG was present which had nonspecifically adhered to the immunoadsorbent column. To prepare soluble immune complexes, antibodies were added to antigens while mixing, at the desired degree of antigen excess (by weight). Complexes were allowed to stabilize at room temperature for 1 hr, then at 4° for 2 hr prior to sucrose density gradient ultracentrifugation, or at 4° overnight prior to analytical ultracentrifugation.

In the studies performed on redissolved complexes, the complexes were allowed to precipitate at equivalence and stabilize overnight at 4°. Then the precipitate was washed four times to remove soluble proteins. Thereafter, antigen was added to the precipitate to yield a final concentration of five times antigen excess. The mixture was incubated overnight at 37° and for a week at 4° with repeated mixing. The solution was centrifuged and further studies carried out on the supernatant containing the soluble complexes. Only 25% of the original antibodies in the precipitate was solubilized under these conditions.

Sucrose Density Gradient Ultracentrifugation. Linear sucrose density gradients (10–30% or 10–40%) were constructed, and the linearity was confirmed periodically by refractometry; 5.8 ml of each sucrose solution was used for construction of gradients, and 0.2 ml of the sample was layered on the top of the gradient. Centrifugation was carried out in a Beckman Model L2B centrifuge, using a Model SW41T rotor, at 40,000 rpm for 15 hr at 4°. The gradients were harvested through a hole in the bottom. Between 30 and 40 fractions were obtained for each gradient. The fractions were analyzed for radioactivity in an automatic well-type γ counter. The ^{125}I counts were corrected for Compton scatter from the ^{131}I present by using standards run with each experiment. The counts per minute were plotted against per cent gradient volume, and the sedimentation coefficient of each major peak was estimated by the short formula method of Martin and Ames (1961). The free antigen peaks were used as the markers for these calculations, utilizing 4.45 S as the sedimentation coefficient for HSA or BSA.

Analytical Ultracentrifugation. Sedimentation velocity experiments were performed according to Schachman (1957) in a Beckman Model E analytical ultracentrifuge using the schlieren optical system with bar angles adjusted so that the complex peaks could be photographed. However, frequently the free antigen peak could not be visualized at the same time. The runs were made at temperatures between 4 and 10°. Viscosity and temperature corrections were made according to Schachman (1957). The expression $\rho = \rho_0 + c(1 - {}^{\phi}v\rho_0)$ was used to calculate the solution density, where c is the concentration in g/ml, ${}^{\phi}v$ is the apparent specific volume, and ρ_0 is the solvent density. The immune complexes were suspended in borate buffer (see above) at protein concentrations between 6.4 and 10.8 mg/ml.

Protein Concentrations. All calculations were based on protein concentrations obtained by absorbance at 280 mμ.

The extinction coefficient ($\epsilon^{1\%}_{1cm}$) for our rabbit antibodies against HSA was determined to be 14.4 by micro-Kjeldahl analysis. The extinction coefficients utilized for the other proteins were: HSA, 6.6; BSA, 6.7; and rhesus antibodies against BSA, 13.7.

Calculation of Ag/Ab Molar Ratios. The following values for molecular weights were utilized: rabbit or rhesus γG, 145,000 (Marler *et al.*, 1964) and HSA or BSA 67,000. From the known protein concentrations and specific activities, the counts per minute per μmole of each antigen or antibody preparation were calculated. In each gradient, the μmoles of antigen or antibody in each fraction, and thus the Ag/Ab molar ratio for each fraction, were calculated.

Calculation of Theoretical Sedimentation Coefficients. In order to calculate the expected sedimentation constants for antigen–antibody complexes, Bloomfield's (1966) generalization of the Kirkwood (1949, 1954) pearl necklace model was used

$$f^{-1} = \left(\sum_{l=1}^{n} \zeta_l\right)^{-1} \left\{1 + \left[6\pi\eta \left(\sum_{l=1}^{n} \zeta_l\right)\right]^{-1} \sum_{\substack{l=1 \\ l\neq s}}^{n} \sum_{s=1}^{n} \zeta_l \zeta_s / L_{ls}\right\} \quad (1)$$

where ζ_l is the translational frictional coefficient of bead l, f is the frictional coefficient of the whole molecule or complex, L_{ls} is the distance between beads l and s, and η is the solvent viscosity.

Initially an attempt was made to obtain a hydrodynamic model of γG which was consistent with previously measured parameters. For this calculation the electron microscopy data of Valentine and Green (1967) and the hydrodynamic data of Noelkin *et al.* (1965) were used. The hydrodynamic data which were used in the calculations are presented in Table I.

Valentine and Green (1967) estimated the anhydrous dimensions of the Fab and Fc fragments by electron microscopy. The axial ratios of the prolate ellipsoids were $p = b/a = 0.583$ and 0.889, respectively; where b is the minor semiaxis and a is the major semiaxis of revolution.

The influence of hydration on frictional coefficient can be taken into account (Oncley, 1941) as

$$f_s = f_{obsd}/(1 + w/\bar{v}\rho)^{1/3} \quad (2)$$

where f_s is the contribution of shape to the frictional coefficient and w is the hydration in grams of solvent/gram of protein; $\bar{v}$ is the partial specific volume of protein, and ρ is solvent density. f_s can be calculated from Perrin's (1936) equations for the axial ratio p as

$$f_s = \frac{6\pi\eta a\sqrt{1 - p^2}}{\ln\left\{(1 + \sqrt{1 - p^2})/p\right\}} \quad (3)$$

Thus, f_s depends on the value of a. However, the anhydrous particle volume is given by

$$V_p = \frac{M\bar{v}}{N} = \frac{4}{3}\pi b^2 a = \frac{4}{3}\pi p^2 a^3 \quad (4)$$

So that the equation used to calculate f_s becomes,

$$f_s = \frac{6\pi\eta\left(\frac{3M\bar{v}}{4\pi N}\right)^{1/3}\sqrt{1 - p^2}}{p^{2/3}\ln\left\{(1 + \sqrt{1 - p^2})/p\right\}} \quad (5)$$

TABLE I: Physical Data Used for the Hydrodynamic Model of γG.

Fragment	M^a (× 10^{-3} g/mole)	$s^0_{20,w}$ (S)	[η] (ml/g)	f_{obsd} (× 10^7 g/sec)
Fab	52	3.8	3.8	0.595
Fc	48	3.8	4.2 ± 0.3	0.549
γG	145	6.7	6.0	0.987

[a] $\bar{V} = 0.738$ was assumed for all data in the table.

In the computer program (FOCAL-12) we entered f_{obsd}, M, $\bar{v}$, and w and then iterated the computation of by p by trial and error. The values of p were then graphed as a function of w for $0.10 \leqslant w \leqslant 0.35$. On the same graph horizontal lines were drawn for the values of p determined by electron microscopy. Figure 1 shows the results of this calculation for the Fab and Fc hydrodynamic values finally used. The horizontal lines labeled EM#1 are the axial ratios determined by Valentine and Green (1967).

Other hydrodynamic data were considered in the calculations (Charlwood and Utsumi, 1969; Pilz *et al.*, 1970), but were not used in the final model because the data of Noelkin *et al.* (1965) were more consistent with the electron microscopy information. The horizontal lines labeled EM#2 in Figure 1 were published after the calculations were made (Labaw and Davies, 1971) and are reasonably consistent with the EM#1 data in terms of the amount of hydration of the fragments.

From the intersection of EM and hydrodynamic data, it was concluded that the Fc fragment was hydrated to the extent of 0.23–0.24 g of solvent/g of protein and the Fab fragment to 0.25–0.28 g of solvent/g of protein.

An attempt was then made to determine the distance separating the subunits of the whole γG molecule according to the method of Charlwood and Utsumi (1969). Equation 1 for this system becomes

$$f_{\gamma G} = \frac{2f_{ab} + f_c}{1 + \frac{1}{3\pi\eta(2f_{ab} + f_c)}\left(\frac{f_{ab}^2}{L_{ab}} + \frac{2f_{ab}f_c}{L_c}\right)} \quad (6)$$

where $f_{\gamma G}$, f_{ab}, and f_c are the frictional coefficients observed for γG, Fab, and Fc, respectively. L_{ab} is the distance between the centers of the Fab fragments and L_c is the distance between the centers of the Fab and Fc fragments (symmetry is assumed). This equation has two unknowns: L_{ab} and L_c. A graph of L_{ab} as a function of L_c is hyperbolic since L_{ab} and L_c are the only variables of eq 6.

It was first thought that a unique model of the γG molecule could be selected by utilizing the viscosity data. However, the frictional coefficient calculated from these data was precisely the same as determined from the sedimentation coefficients.

All of the distances obtained by eq 6 satisfy exactly the same sedimentation coefficient; however, not all are reasonable structures. From a graphic representation of the structures, it was observed that the only reasonable values were L_c between 70 and 80 Å, and therefore L_{ab} between 112 and 82 Å. At larger L_c, the Fab fragments were too far separated from the Fc fragment to be reasonable. At smaller values of L_c, the Fab fragments would have occupied the same space as the Fc fragments.

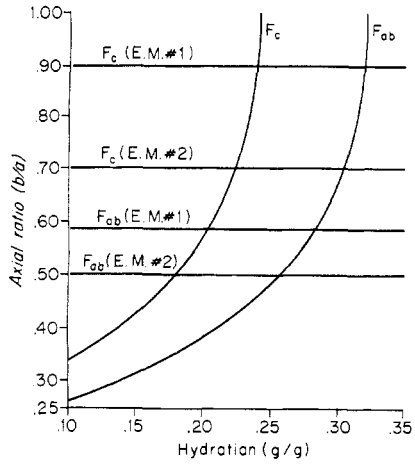

FIGURE 1: Axial ratio as a function of hydration computed from the sedimentation data of Noelkin *et al.* (1965) (curved lines). The lines labeled EM#1 are from the axial ratio published by Valentine and Green (1967). The EM#2 lines are from Labaw and Davies (1971).

Figure 2 depicts the three structures which were considered reasonable (at 5-Å increments in L_c). Since the Fab and Fc fragments are considered as point sources of friction in the hydrodynamic calculations, the orientations of the three fragments cannot be determined. Consequently, the models were drawn based on the fact that the molecule can assume both a Y shape (Valentine and Green, 1967) and a T shape (Pilz *et al.*, 1970). However, only models 1 and 2 were used in the calculation of sedimentation coefficients of BSA–anti-BSA complexes.

From these calculations, we predicted for Fc an ellipsoid with a = 31.6 Å, b = 24.1 Å, $w \simeq 0.24$ g/g; and for Fab a = 40 Å, b = 23 Å, $w \simeq 0.27$ g/g. After this calculation was completed, more electron microscopy data and an X-ray diffraction study of a γG molecule were published (Sarma *et al.*, 1971). If the X-ray data are converted to ellipsoids of revolution, for Fc one can calculate a = 32 Å, b = 20.7 Å; and for Fab, a = 35 Å, b = 22.4 Å. Thus, we concluded that the hydrodynamic calculations were in reasonable agreement with the shape of the γG molecule as determined by a variety of methods.

Calculation of the Frictional Resistance of BSA. Various attempts were made to model BSA as three spheres as was done by Bloomfield (1966) for the low pH behavior of the molecule. Since neither reliable electron microscopy data nor X-ray data exist for this molecule, we attempted to find a

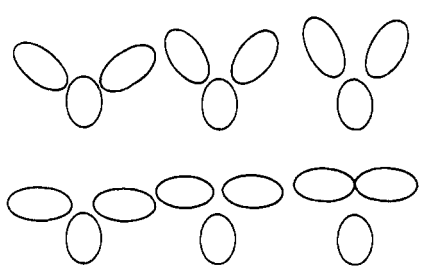

FIGURE 2: Three reasonable models of γG derived from hydrodynamic data. The models on the top correspond to Y shapes but have the same hydrodynamic properties as the T shapes in the bottom row. The models are numbered 1, 2, 3, proceeding from left to right in the figure.

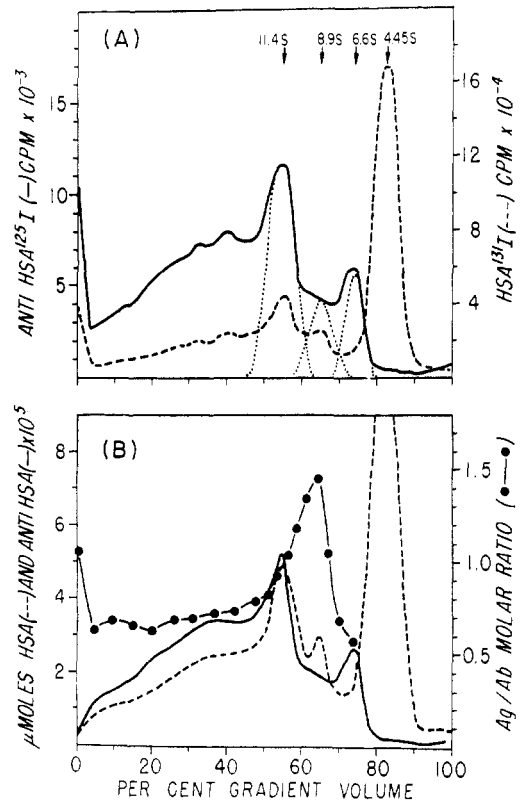

FIGURE 3: Sucrose density gradient pattern of HSA-^{131}I–anti-HSA-^{125}I complexes prepared at five times antigen excess. (A) Counts per minute of HSA-^{131}I (- - -) and of anti-HSA-^{125}I (——) were plotted against per cent gradient volume (0% bottom and 100% top of the gradient). Partial resolution of the immune complex distribution pattern into its component curves, as determined by a Du Pont 310 curve resolver, is shown by the dotted lines (· · · ·). (B) Micromoles of HSA (- - -) and of anti-HSA (——), and Ag/Ab molar ratio (·—·) *vs.* per cent gradient volume. The estimated sedimentation coefficients for each major peak of both graphs are given at the top of graph A.

three-sphere solution from hydrodynamic data alone. The parameters used were: M = 67,000 g/mole, $\bar{v}$ = 0.734 ml/g (Dayhoff *et al.*, 1952), s = 4.45 S (Harrington *et al.*, 1956), and $[\eta]$ = 3.704 ml/g (Tanford and Buzzell, 1956). No physically reasonable solution could be found for the simultaneous solution of the sedimentation and viscosity data. For the treatment of the viscosity data, eq 17 of Bloomfield (1966) was used. This procedure was utilized instead of the one used for γG, since $\beta = 2.07 \times 10^7$ from sedimentation and viscosity data. This value is less than should be found theoretically; it either represents a breakdown of the theory of the equivalent sphere (Tanford and Buzzell, 1954), a compensation of errors in theory which occasionally can be treated as in eq 8 *et sequens*, or experimental errors of measurement of physical constants. In any case, we were forced to consider the BSA molecule as an ellipsoid of revolution, a prolate ellipsoid with b = 18.6 Å, a = 67.7 Å, w = 0.15 g/g. These dimensions agree very well with the calculations of Squire *et al.* (1968). The data for HSA are within experimental error of the BSA parameters (Smith, 1968), so that the same shape was used for this protein.

Results

HSA–Anti-HSA Complexes. HSA-^{131}I–anti-HSA-^{125}I complexes were prepared at 5 times, 20 times, 40 times, and 100 times antigen excess by weight, using antibodies obtained

TABLE II: Estimated Sedimentation Coefficients (by Sucrose Density Gradients)[a] and Molar Ag/Ab Ratios of the Major Peaks of Immune Complexes Prepared in Antigen Excess.

	$s_{20,w}$[b]	Molar Ratio[b]	$s_{20,w}$[b]	Molar Ratio[b]
	A. HSA–Anti-HSA Complexes			
Five times antigen excess[c]	11.0 ± 0.4	0.85 ± 0.08	8.5 ± 0.3	1.24 ± 0.18
Twenty times antigen excess	10.8	0.95	8.5	1.80
Forty times antigen excess	10.8	0.93	8.6	1.75
One-hundred times antigen excess	10.8	0.93	8.6	1.77
	B. BSA–Anti-BSA Complexes			
Five times antigen excess[d]	10.7 ± 0.3	1.03 ± 0.06	8.5 ± 0.2	1.17 ± 0.05
Twenty times antigen excess	10.6	1.32	8.8	1.48

[a] Estimated from HSA or BSA marker of 4.45 S. [b] Mean ± 1 SD, when based on multiple determinations. [c] Six separate determinations. [d] Two separate determinations.

from rabbits hyperimmunized with HSA in complete Freund's adjuvant. Sucrose density gradient separations were performed on all of these complexes and analytical ultracentrifugation analysis carried out on two.

The sucrose density gradient patterns of HSA-anti-HSA complexes prepared at 5 times antigen excess (Figure 3) showed a peak of free antigen, one of free antibodies, two identifiable peaks of immune complexes and a population of complexes of larger sizes. One peak of complexes was discernible with a sedimentation coefficient of about 8.5 S and a larger clear-cut peak of about 11 S.[2]

The Ag/Ab molar ratios for each sucrose density gradient fraction are shown in Figure 3B for HSA–anti-HSA complexes made at 5 times antigen excess. Proceeding from large to small complexes, the molar ratio of the larger complexes rose from 0.6 to 0.8, and then approached 1.0 as the 11S complex peak was reached. The molar ratio then rose towards the 8.5S peak, and fell as the free antibody peak was reached. The molar ratio of the 11S complexes, in the preparations made at five times antigen excess, was 0.85 ± 0.08 (Table II), and for the 8.5S complexes was 1.24 ± 0.18.

In order to determine more accurately the molar ratios of these peaks without an interfering 6.6S antibody peak, complexes were prepared by redissolving the washed precipitate at five times antigen excess. The sucrose density gradient analysis of these complexes (Figure 4) showed that the heavier peak had a molar ratio of 0.85, and the lighter peak a ratio of 1.25. When the μmoles of HSA and of anti-HSA were plotted, rather than the counts as shown in Figure 4, the free antigen peak was seen to be 20 times the size of the antigen peak in the 8.5S complexes. A Gaussian distribution of the free antigen peak was determined both by curve resolver and by a sucrose density gradient pattern of HSA run alone. The leading edge of the free antigen peak in the complex mixture was extrapolated and was seen to extend partially under the 8.5S complexes. When the antigen in these complexes was corrected by the amount of free antigen present, the molar ratio approached 1.0.

Sucrose density gradient analysis of HSA–anti-HSA complexes prepared at 20, 40, and 100 times antigen excess showed the presence of the same two complex peaks, with the 11S peak predominating. The molar ratio of this peak was 0.94 and that of the 8.5S peak 1.77 (see Table II). However, because of the very large amount of free antigen present, accurate corrections of the 8.5S peaks for the contributions by the leading edges of the free antigen peaks could not be made. Therefore, it was possible that the 8.5S complexes contained a mixture of 1:1 and 2:1 complexes with the former greatly predominating at low to moderate degrees of antigen excess and the latter increasing in amount at extreme degrees of antigen excess.

The results of analytical ultracentrifugation of HSA–anti-HSA complexes are shown in Table III and Figure 5. A peak of 8.7 S to 9.3 S and a peak of 11.5 S to 12.0 S were found, in comparison with the values found by sucrose density gradient of 8.5 S and 11.0 S. The 8.7S to 9.3S peak was predominant here; while by sucrose density gradient analysis the 11.0S peak was the major peak. This suggested that during the zonal separation in the sucrose gradient, some of the 8.5S complexes may have dissociated into free antigen and antibodies, or possibly dimerized to form 11S complexes. The absence of a discrete free antibody peak in the analytical ultracentrifuge suggested that dissociation may have occurred to some degree in the preparative centrifuge. However, the absence of a free antibody peak in the complexes redissolved from precipitate indicated that this possible dissociation was

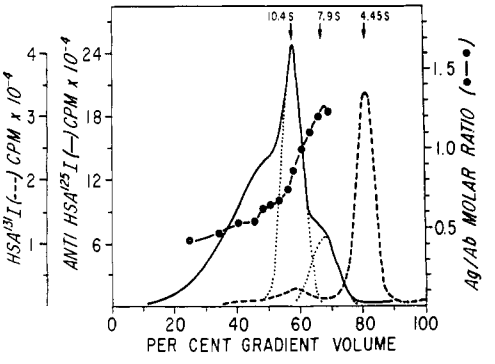

FIGURE 4: Sucrose density gradient pattern of HSA-^{131}I–anti-HSA-^{125}I complexes redissolved from precipitate at fivefold antigen excess. Counts per minute of HSA-^{131}I (--) and of anti-HSA-^{125}I (—) and the Ag/Ab molar ratio (·—·) *vs.* per cent gradient volume. Component curves are shown by the dotted lines (····).

[2] Subsequently in the text, these peaks will be termed 8.5 S and 11 S, although the actual values found in the individual gradient were recorded in the figures.

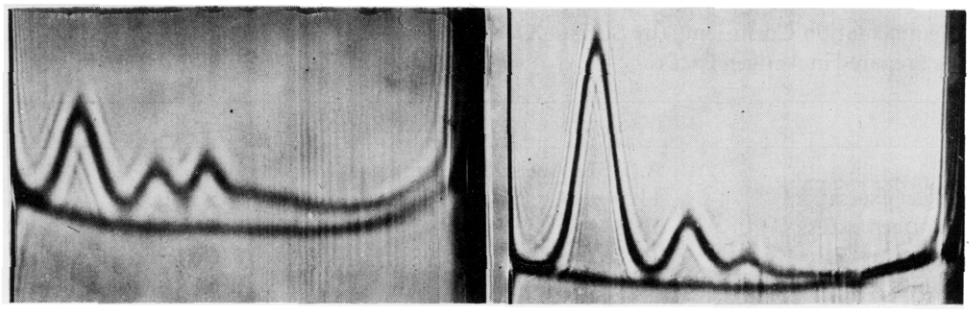

FIGURE 5: Analytical ultracentrifugation analysis of HSA–anti-HSA complexes prepared at five times (left) and twenty times (right) antigen excess. The direction of centrifugation is from left to right. In both patterns the peak at left represents free antigen and the subsequent peaks are immune complexes. The patterns for BSA–anti-BSA complexes were similar.

minimal. It is also possible that under the nonequilibrium conditions of the preparative centrifuge the Ag_2Ab_1 complexes may have dissociated to Ag_1Ab_1. However, evidence will be presented to indicate that this dissociation was unlikely.

In order to examine complexes formed with antibodies of low affinity, HSA-^{131}I–anti-HSA-^{125}I complexes were prepared using antibodies obtained from early bleedings of rabbits after IV immunization (see Methods). During the isolation of these antibodies, the immunoadsorbent columns were not fully saturated; this served to insure that low affinity antibodies would not be selectively displaced from the columns. At equivalence only 17% of these antibodies were precipitated. Sucrose density gradients analysis of the supernatant from the point of equivalence showed some 11S and 8.5S complex formation, suggesting the presence of nonprecipitating antibodies. Soluble complexes were prepared at 5 times or at 20 times antigen excess, thus utilizing both precipitating and nonprecipitating antibodies. Complexes were also obtained by precipitating the antibodies at equivalence and dissolving the washed precipitate at five times antigen excess. Sucrose density gradient patterns were obtained on complexes prepared by both methods. The estimated sedimentation coefficients and the Ag/Ab molar ratios of these limiting complexes were the same as for complexes made with antibodies purified from hyperimmunized rabbits. Thus it appeared that the route of immunization, use of complete Freund's adjuvant, length of immunization, and possible presence or absence of nonprecipitating antibodies did not affect the nature of the limiting soluble complexes formed in these systems.

In summary, study of HSA–anti-HSA complexes in low to moderate degrees of antigen excess showed two major limiting peaks. The smaller peak was 8.5 S by sucrose density gradient, and 9.0 S by analytical ultracentrifugation, with a molecular composition of primarily Ag_1Ab_1. The larger peak was 11.0 S by sucrose density gradient and 11.7 S by analytical ultracentrifugation with a molecular composition of Ag_2Ab_2.

BSA–Anti-BSA Complexes. BSA–anti-BSA complexes were prepared at 5 and 20 times antigen excess, using antibodies isolated from rhesus monkeys. The sucrose density gradient patterns of complexes prepared at five times antigen excess showed two major complex peaks of 8.5 ± 0.2 S and 10.7 ± 0.3 S, with Ag/Ab molar ratios of 1.17 ± 0.05 and 1.03 ± 0.06, respectively (Table II). Again the molar ratio of the 8.5S complexes was falsely elevated by the leading edge of the large free antigen peak.

By analytical ultracentrifugation, the two complex peaks were 9.0 S and 11.6 S to 12.2 S (see Table III). At both 5 and at 20 times antigen excess, the lighter peak predominated over the heavier complex peak. Thus the BSA–anti-BSA complexes appeared to have sedimentation characteristics and molecular composition similar to those of the HSA–anti-HSA complexes. The 11S complexes were primarily Ag_2Ab_2 and the 8.5S complexes mainly Ag_1Ab_1.

Calculation of the Theoretical Sedimentation Coefficients for Antigen–Antibody Complexes. Since many antigenic sites exist on the multivalent BSA (or HSA) molecule, an attempt was made to calculate the sedimentation coefficient distribution for 1:1 and 2:1 complexes of antigen and antibody. Antibody models 1 and 2 in Figure 2 were used under the following conditions: (1) a Y-shaped antibody molecule with binding site on the vector drawn between the center of the Fc and Fab fragments, (2) a T-shaped antibody with the binding site at the extreme end of the vector between Fab fragments, and (3) a Y-shaped molecule with the binding site at the maximum y coordinate of the Fab ellipsoid (y is the vertical and x is the horizontal coordinate of the ellipsoids

TABLE III: Sedimentation Coefficients, Determined by Analytical Ultracentrifugation, of Immune Complexes Prepared in Antigen Excess.

	$s_{20,w}$	% of Total Protein
A. HSA–Anti-HSA Complexes		
Five times antigen excess[a]	4.39	45
	9.30	20
	11.96	19
	>11.96	16
Twenty times antigen excess	4.25	69
	8.67	18
	11.48	9
	>11.48	4
B. BSA–Anti-BSA complexes		
Five times antigen excess	4.32	18
	8.99	26
	12.19	19
	>12.19	37
Twenty times antigen excess	4.67	52
	9.05	22
	11.6	15
	>11.6	11

[a] Average of two separate determinations.

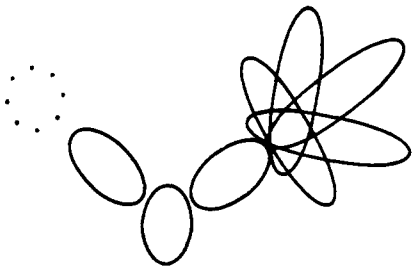

FIGURE 6: BSA–anti-BSA complex for Y-shaped antibody model 1 of Figure 2. The antibody binding site is considered to be on the vector between the centers of the Fc and Fab fragments. The four ellipsoids on the right of the antibody molecule depict some of the assumed orientations of the BSA molecule. The circle of dots on the left are the loci of centers of the BSA molecule attached to this Fab fragment.

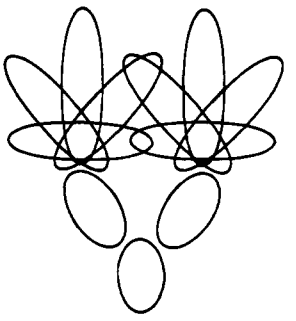

FIGURE 7: BSA–anti-BSA complex for Y-shaped antibody model 2 of Figure 2. The binding site is considered to occur at the maximum y coordinate of the Fab ellipsoids. The overlapping BSA ellipsoids indicate structures which cannot physically exist and such combinations represent obligatory 1:1 antigen–antibody complexes.

shown in Figure 2). The BSA (or HSA) was considered to have antigenic sites at every point on its surface and displaced 5 Å from the binding site of the antibody. The 1:1 complexes were called optional if they were sterically capable of containing another antigen to form 2:1 complexes; they were termed obligatory if the configuration did not allow placement of another antigen. The three models will be considered in order.

(1) The Y-shaped antibody molecule with the BSA antigen is shown in Figure 6. For 1:1 complexes of this type, the mean sedimentation coefficient was 7.76 S with standard deviation 0.26 S (see Table IV). For 2:1 complexes, these values were 8.64 S ± 0.44 S.

(2) The T-shaped antibody molecule together with the BSA antigen yielded almost precisely the same values for sedimentation constant as the Y-shaped model. For 1:1 complexes, the values were 7.77 S ± 0.26 S, and for 2:1 complexes, 8.63 S ± 0.45 S (see Table IV). The maximum deviation between comparable orientations of the BSA molecule as Y and T shapes was 0.15 S. Thus, the distribution of sedimentation coefficients was not very sensitive to the conformation of the antibody.

(3) When a Y-shaped antibody molecule was assumed with binding site at maximum y coordinate (Figure 7), then certain orientations of the antigen were disallowed due to steric overlap. Excluding these models with steric hindrance, the 2:1 complexes were predicted to have a sedimentation coefficient of 8.97 S ± 0.40 S (see Table IV). 1:1 complexes were calculated (see Figure 8) so that they could not bind another antigen due to steric overlap. Twenty-one such obligatory Ag_1Ab_1 models were generated; these had a mean sedimentation coefficient of 8.35 S and standard deviation of 0.20 S (Table IV). For these models the gap between the antibody binding site and the BSA varied, as may be discerned in Figure 8, but the complexes were sterically incapable of containing two antigen molecules.

Sedimentation coefficients were also calculated for Ag_1Ab_1 complexes in which the BSA (HSA) molecule spanned both of the antibody binding sites. The sedimentation coefficients for these compact Ag_1Ab_1 models were 9.65 S, 8.89 S and 8.65 S, respectively, using the three Y-shaped antibody molecules in Figure 2.

Discussion

The results of these studies indicated that the composition of the smallest limiting soluble complexes in low to moderate degrees of antigen excess was principally Ag_1Ab_1, in both the HSA–anti-HSA and the BSA–anti-BSA systems. As pointed out in the introduction, other investigators had indicated that Ag_2Ab_1 was the composition of the limiting complex with the same antigen–antibody systems. In the current work we determined molar ratios of antigens and antibodies after separation of the complexes by zonal ultracentrifugation. Analytical ultracentrifugation was carried out on the same preparations to avoid possible dissociation and to compare our observations with results obtained by others. A computer model was constructed for calculation of theoretical sedimentation co-

TABLE IV: Theoretical Sedimentation Coefficients of Soluble Immune Complexes.

Complex	$s_{20,w}$ Mean ± 1 SD (Range)
Y-Shaped Antibody	
Ag_1Ab_1 (optional)	7.76 ± 0.26 (7.47–8.16)
Ag_2Ab_1	8.64 ± 0.44 (8.14–9.33)
T-Shaped Antibody	
Ag_1Ab_1 (optional)	7.77 ± 0.26 (7.48–8.19)
Ag_2Ab_1	8.63 ± 0.45 (8.13–9.35)
Y-Shaped Antibody, Binding Site at y_{max}	
Ag_1Ab_1 (obligatory)	8.35 ± 0.20 (8.03–8.65)
Ag_2Ab_1	8.97 ± 0.40 (8.60–9.90)

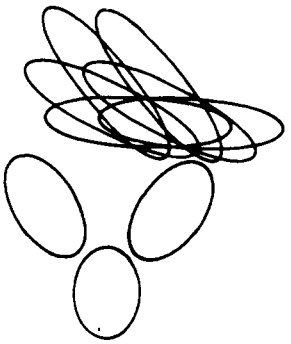

FIGURE 8: BSA–anti-BSA complex for Y-shaped antibody model 2 of Figure 2 in various orientations which exclude 2:1 Ag/Ab ratios. The horizontal BSA molecule was translated to the left to test the hydrodynamic theory as described in the text.

efficients and used to evaluate the influence of various arrangements of the antigen and antibody on the sedimentation coefficients of the limiting complexes.

Two potential problems in our methodology should be considered in comparison with previous investigations. (1) Could the combining properties of the antibodies have been altered by the elution from immunoadsorbents? (2) Did dissociation of complexes occur during zonal centrifugation when they were removed from the environment of antigen excess?

A possible alteration in the combining properties of antibodies isolated by the immunoadsorbent techniques appeared unlikely for several reasons. The catabolic rate of these antibodies (Mannik *et al.*, 1971) was no different than that of rabbit γG isolated by gentle procedures, suggesting no alterations in the Fc portion of the molecule. Furthermore, soluble complexes made from radiolabeled antigen and pooled antisera showed the presence of 11S and 8.5S complex peaks by sucrose density gradient, although the molar ratios of these complexes could not be determined (W. P. Arend, unpublished data). In addition, recent studies on antibody molecules recombined from isolated heavy and light chains showed no change in the antibody valence or binding constant, when the heavy and light chains were from the original parent molecule (Bridges and Little, 1971). In the latter experiments the polypeptide chains were exposed to perturbants of comparable nature as those used in our experiments for isolation of intact antibodies. Therefore, it appears unlikely that any significant irreversible damage occurred to antibodies used in our studies.

Some conversion of Ag_1Ab_1 complexes to Ag_2Ab_2 complexes, or *vice versa*, could have occurred during zonal centrifugation. However, it is unlikely that significant dissociation of Ag_2Ab_1 complexes to Ag_1Ab_1 complexes occurred. ΔH is small for complex formation (Singer and Campbell, 1955); thus little dissociation could be expected as a result of temperature changes. Also, the reactions of association are fast while those of dissociation are slow for antigen–antibody complexes. The distribution of sedimentation coefficients of the preparations made by redissolved complexes was essentially the same as those made by addition of the antibody. Complexes made from a pool high in nonprecipitating antibodies (also probably antibodies of low affinity) did not alter the sedimentation constants. Furthermore, there was no evidence of the presence of a significant amount of 7.76S material, by either sucrose density gradient or analytical ultracentrifugation, indicating that the optional 1:1 complexes were not present. These observations all support the conclusions that the Ag_1Ab_1 complexes were formed directly, and did not result from dissociation of Ag_2Ab_1 complexes.

The sedimentation coefficients determined by analytical ultracentrifugation were slightly higher than the values obtained by zonal centrifugation. The latter values were calculated by the short method of Martin and Ames (1961), which assumes spherical shape for the sedimenting protein, a property probably not characteristic of soluble antigen–antibody complexes. The values of 8.5 S and 11.0 S for the two limiting complex peaks, determined by zonal centrifugation, and 9.0 S and 11.7 S, determined by analytical ultracentrifugation, closely approximate the values obtained by other workers for the same antigen–antibody systems. Thus it is likely that the complexes studied in these experiments are identical with those studied by others.

The calculations of theoretical sedimentation coefficients on the models of immune complexes indicated several important points, even though the site(s) of antigenic determinants of BSA (HSA) and the combining site of the antibody are not known. A range of sedimentation coefficients was found for each model complex (Table IV), because of the multiple possible sites of antigenic determinants on the BSA (HSA) molecule and the variable spatial relationship to the antibody. More important, however, was the finding that the mean calculated sedimentation coefficients of complexes with differing molar composition can be so close that individual boundries would not be discernible by schlieren optics because of the effect of diffusion. Complexes with two or more antibodies—*e.g.*, Ag_1Ab_2, Ag_2Ab_2, etc.—would have an even broader range of sedimentation coefficients, since more rotations and translations of the molecules are possible. Another valuable observation from these calculations was that the Ag_1Ab_1 complexes potentially can have sedimentation coefficients which are quite similar to Ag_2Ab_1 complexes. If the antigen in the Ag_1Ab_1 complex was positioned so that interaction with a second antigen was possible (an optional 1:1 complex), the expected sedimentation coefficient was 7.76 S. If the antigen in the Ag_1Ab_1 complex was positioned so that placement of a second antigen was not sterically possible (an obligatory 1:1 complex), the expected sedimentation coefficient was 8.35 S. If the antigen molecule spanned both antibody binding sites, the expected sedimentation coefficients were 8.65 S to 9.65 S. The observed sedimentation coefficient of this complex peak was 8.5 S by sucrose density gradient and 9.0 S by analytical ultracentrifugation. Even though this peak may have represented the summation of Gaussian distributions of two or more components, it is probable that little material was present with a sedimentation constant as low as 7.76 S. Therefore we concluded that the 1:1 complexes present were obligatory and were of a compact composition with the antigen probably spanning both binding sites. These observations support recent theoretical considerations which concluded that the reaction of a single bivalent γG antibody molecule with a single multivalent protein antigen should predominate over the reaction with two antigen molecules (Crothers and Metzger, 1972).

The validity of the model used for calculation of theoretical sedimentation coefficients needs some discussion. The model used for antibodies agrees with most of the available data on the shape and hydration of this molecule (see Materials and Methods). The model for BSA is less satisfactory, but does agree with the hydrodynamic data. The assumptions used in modeling the complex are tenuous since neither the location of the antibody binding site nor the location of the antigenic determinants on the BSA (HSA) is known. For these reasons the calculations were carried out with two different conformations of the antibody, with a variation in the location of the binding site, in addition to translation and rotation of the antigen across the binding site. The calculated sedimentation coefficients based on this model do agree with published sedimentation coefficients of 7.7 S for the optional Ag_1Ab_1 and 8.9 S for the Ag_2Ab_1 complexes (Lapresle and Webb, 1965). In the latter experiments these complexes were achieved by isolation of antibodies that recognized only limited antigenic determinants on the HSA molecule. Calculations of the Ag_1Ab_1 model caused additional difficulties. Zwanig *et al.* (1968) showed that singularities occur in the frictional interaction matrix under strong conditions of hydrodynamic interaction, leading to nonphysical values of the frictional coefficient under these conditions. To test whether the sedimentation coefficients calculated for the model antigen–antibody complexes were reasonable, the models were tested

in the following way. The BSA model was placed perpendicular to the symmetry axis of the antibody with binding site at the maximum y coordinate. It was then translated along the x axis by small (1 Å) steps toward the symmetry axis and sedimentation coefficients were calculated at each step. The result was that as the molecule moved toward the symmetry axis, sedimentation coefficients increased, as they should. However, a maximum was observed as well as an inflection point as the center of the BSA molecule moved toward the symmetry axis. This behavior of the model does not seem reasonable–as the complex becomes more compact, its sedimentation coefficient should increase rather than decrease. Putting this theoretical problem aside, on thermodynamic considerations both antibody binding sites in the Ag_1Ab_1 complexes should have interacted with the antigen molecule. The calculated sedimentation coefficients for the Ag_1Ab_1 models in which the antigen spanned both binding sites closely approximated the values observed by ultracentrifugation. Actually, these calculated values may have been slightly low because of the theoretical difficulties with the Ag_1Ab_1 model.

In several published studies concerning the molar ratio of the limiting soluble complexes in the BSA–anti-BSA or HSA–anti-HSA systems, including the work of Singer and Campbell (1952), the amount of free antigen in soluble complex solutions was estimated from the schlieren patterns of analytical ultracentrifugation or from ascending electrophoresis patterns. With progressive increase in antigen excess the Ag/Ab molar ratio of the smallest (8.7 S) complexes increased from 0.92 to 1.24 (Singer and Campbell, 1952). Recalculation of these data with a molecular weight of 145,000 for rabbit γG lowers these values to 0.83 and 1.12, respectively. Of more concern is the possible contribution of the free HSA or BSA to this small peak of complexes, particularly in that higher concentrations of antigen excess progressively increased the Ag/Ab molar ratio in total complexes to 2.81 when free electrophoresis was used to determine the amount of unbound antigen (Plescia *et al.*, 1952). Furthermore, electrophoresis in starch medium showed that the Ag/Ab molar ratio rose from 0.75 to 8.9 as the Gaussian distribution of free antigen falsely elevated the amount of antigen under the peak of complexes (Ishizaka *et al.*, 1959). These observations clearly reflect the error inherent in the estimation of free antigen from schlieren patterns. Similarly, the leading edge of the free antigen peak falsely elevated the molar ratio of the 8.5S complexes in our studies. This point was best illustrated in experiments with soluble complexes prepared from an immune precipitate. Thus, the average Ag/Ab ratio of 1.24 ± 0.18 in the Ag_1Ab_1 complexes is higher than the true value. If these small limiting complexes were Ag_2Ab_1, the observed molar ratio should have exceeded 2.0. Therefore, the predominant complex in the 8.5S peak must have been Ag_1Ab_1, but we could not exclude the presence of a small amount of Ag_2Ab_1 complexes.

In previous studies the presence of Ag_1Ab_1 complexes in the BSA–anti-BSA system was dismissed since no further separation of the smallest complexes was seen by free electrophoresis (Singer and Campbell, 1952). However, adequate separation of Ag_1Ab_1 and Ag_2Ab_1 complexes has not been demonstrated by this technique. Furthermore, electrophoretic separation could not be expected if in fact the complexes were primarily Ag_1Ab_1, as shown by our observations. Previous investigations of this problem also have not utilized aggregate-free antigen preparations. The molar ratios of the potential complexes formed between aggregated albumin and antibodies may have greatly influenced the conclusions that were reached. The agreement of sedimentation coefficients of the Ag_1Ab_1 and Ag_2Ab_2 in the current study with the sedimentation coefficients observed previously by others in similar systems indicates that the antibody preparations were comparable and the problems outlined above resulted in conclusions different from those reached by us. In an earlier investigation (Mannik *et al.*, 1971) the 11.0S complexes in the HSA–anti-HSA system were thought to be composed of Ag_1Ab_2 complexes because the amount of antigen present was underestimated at that time.

Weigle and Maurer (1957) used guinea pig complement to precipitate soluble antigen–antibody complexes and determined that the Ag/Ab molar ratio of these complexes approached 2 as antigen excess was increased. However, it has subsequently been shown that soluble immune complexes containing less than three antibody molecules do not fix complement (Hyslop *et al.*, 1970; Mannik *et al.*, 1971). Thus the material precipitated by complement in the studies of Weigle and Maurer (1957) was not the limiting complexes, which possess two or one antibody molecule. Mulligan *et al.* (1966), utilized the Farr antibody combining technique to study this problem, separating the limiting complexes from free antigen by 50% ammonium sulfate precipitation at extreme degrees of antigen excess. The amount of antigen in the precipitated complexes plateaued at a level giving an Ag/Ab molar ratio of approximately 2 at various amounts of antibody. However, the background subtraction (amount of antigen precipitated by normal rabbit serum and 50% ammonium sulfate) in these studies was very high—between 25 and 90% of the antigen precipitated by the antisera. Also, an average molecular weight for HSA of 83,000 (monomeric and aggregated) was utilized in their calculations.

The methods used in this paper, namely specific activity of labeled antigens and antibodies, appear to be the best present method of studying the molecular composition of limiting complexes for multivalent antigens. The only method which might be as good is electron microscopy (Feinstein and Rowe, 1965). However, the electron microscope preparations must be at a low protein dilution and are washed, dried, and stained prior to analysis, possibly perturbing the chemical equilibria. These techniques have been successfully applied to studying the complexes formed between antibody and divalent hapten (Hyslop *et al.*, 1970), showing the tendency to form cyclic structures. Similar cyclic structures were probably present in our studies. The question of the composition of small soluble complexes should be studied in other antigen–antibody systems, as the conclusions reached in these studies may not be applicable to other multivalent antigens and their antibodies.

Acknowledgments

We thank Anne Grant and David Trout for their technical assistance.

References

Arend, W. P., and Mannik, M. (1971), *J. Immunol. 107*, 63.
Bloomfield, V. A. (1966), *Biochemistry 5*, 684.
Bridges, S. H., and Little, J. R. (1971), *Biochemistry 10*, 2525.
Charlwood, P. A., and Utsumi, S. (1969), *Biochem. J. 112*, 357.
Crothers, D. M., and Metzger, H. (1972), *Immunochemistry 9*, 341.
Dayhoff, M. O., Perlmann, G. E., and MacInnes, R. H. (1952), *J. Amer. Chem. Soc. 74*, 2515.

Feinstein, A., and Rowe, A. J. (1965), *Nature (London) 205*, 147.
Harrington, M. F., Johnson, P., and Ottewill, R. H. (1956), *Biochem. J. 62*, 569.
Helmkamp, R. W., Gooland, R. L., Bale, W. F., Spar, J. L., and Mutschler, L. E. (1960), *Cancer Res. 20*, 1495.
Hyslop, N. E., Jr., Dourmashkin, R. R., Green, N. M., and Porter, R. R. (1970), *J. Exp. Med. 131*, 783.
Ishizaka, K. (1963), *Progr. Allergy 7*, 32.
Ishizaka, K., Ishizaka, T., and Campbell, D. H. (1959), *J. Exp. Med. 109*, 127.
Kirkwood, J. G. (1949), *Recl. Trav. Chim. Pays-Bas 68*, 649.
Kirkwood, J. G. (1954), *J. Polym. Sci. 12*, 1.
Labaw, L. W., and Davies, D. R. (1971), *J. Biol. Chem. 246*, 3760.
Lapresle, C., and Webb, T. (1965), *Biochem. J. 95*, 245.
Mannik, M., and Arend, W. P. (1971), *J. Exp. Med. 134*, 19s.
Mannik, M., Arend, W. P., Hall, A. P., and Gilliland, B. C. (1971), *J. Exp. Med. 133*, 713.
Mannik, M., and Stage, D. E. (1971), *J. Immunol. 106*, 1670.
Marler, E., Nelson, C. A., and Tanford, C. (1964), *Biochemistry 3*, 279.
Martin, R. G., and Ames, B. N. (1961), *J. Biol. Chem. 236*, 1372.
Mulligan, J. J., Jr., Osler, A. G., and Rodriques, E. (1966), *J. Immunol. 96*, 324.
Noelkin, M. E., Nelson, C. A., Buckley, C. E., and Tanford, C. (1965), *J. Biol. Chem. 240*, 218.
Oncley, J. L. (1941), *Ann. N. Y. Acad. Sci. 41*, 121.
Perrin, R. (1936), *J. Phys. Radium 7*, 1.
Pilz, I., Puchwein, G., Kratky, O., Herbst, M., Haager, O., Gall, W. E., and Edelman, G. M. (1970), *Biochemistry 9*, 211.
Plescia, O. J., Becker, E. L., and Williams, J. W. (1952), *J. Amer. Chem. Soc. 74*, 1362.
Sarma, V. R., Silverton, E. W., Davies, D. R., and Terry, W. D. (1971), *J. Biol. Chem. 246*, 3752.
Schachman, H. K. (1957), *Methods Enzymol. 4*, 32.
Singer, S. J., and Campbell, D. H. (1952), *J. Amer. Chem. Soc. 74*, 1794.
Singer, S. J., and Campbell, D. H. (1955), *J. Amer. Chem. Soc. 77*, 3499.
Smith, M. H. (1968), *in* Handbook of Biochemistry, Sober, H. A., Ed., Chemical Rubber Co., Cleveland, Ohio.
Squire, P. G., Moser, P., and O'Konski, C. T. (1968), *Biochemistry 7*, 4261.
Tanford, C., and Buzzell, J. G. (1954), *J. Amer. Chem. Soc. 76*, 3357.
Tanford, C., and Buzzell, J. G. (1956), *J. Phys. Chem. 60*, 225.
Valentine, R. C., and Green, N. M. (1967), *J. Mol. Biol. 27*, 615.
Weigle, W. O., and Maurer, P. H. (1957), *J. Immunol. 79*, 223.
Zwanig, R., Kieffer, J., and Weiss, G. H. (1968), *Proc. Nat. Acad. Sci. U. S. 60*, 381.

Microenvironmental Effects on Enzyme Catalysis. A Kinetic Study of Polyanionic and Polycationic Derivatives of Chymotrypsin†

Leon Goldstein

ABSTRACT: A series of water-soluble polyanionic and polycationic derivatives of chymotrypsin were prepared by growing poly(glutamyl) or poly(ornithyl) side chains on the enzyme, by coupling chymotrypsin to an ethylene–maleic acid copolymer (EMA) and by partial succinylation or acetylation. The pH–activity profiles of the polyanionic derivatives of chymotrypsin were displaced toward more alkaline pH values as compared to the native enzyme; conversely the pH–activity profiles of the polycationic derivatives were displaced toward more acidic pH values. The k_{cat} values of the charged chymotrypsin derivatives acting on ester, amide, and anilide substrates were displaced symmetrically, relative to the native enzyme—to higher values in the case of the polyanionic derivatives (poly(glutamyl)chymotrypsin, EMA–chymotrypsin, succinylchymotrypsin, and acetylchymotrypsin), and to lower values in the case of the polycationic (poly(ornithyl)chymotrypsin) derivatives. The electrostatic effects on k_{cat} were much more pronounced when the substrate was amide or anilide than when it was an ester. Increasing the ionic strength caused an increase in the values of k_{cat} of both native chymotrypsin and the positively charged derivatives of the enzyme. The k_{cat} values of the negatively charged derivatives were not affected by the ionic strength. With ester substrates the values of K_m(app) of the polycationic derivatives were higher by an order of magnitude in comparison to the native enzyme; the K_m(app) values of the polyanionic derivatives were only slightly perturbed. The values of K_m(app) of all chymotrypsin derivatives acting on amide and anilide substrates were unperturbed and essentially identical with the value of the Michaelis constant of the native enzyme. These findings are discussed in the light of some recent ideas regarding the mechanism of action of chymotrypsin.

Studies on water-insoluble derivatives of several enzymes, in which the biologically active protein is covalently bound to a high molecular weight support material, have shown that the chemical nature, and in particular the charge of the carrier polymer, have a profound effect on both the stability and the overall kinetic behavior of the enzyme derivative (Goldstein

† From the Department of Biochemistry, Tel-Aviv University, Tel-Aviv, Israel. *Received April 4, 1972.* Part of the experimental work described in this article was carried out at the Weizmann Institute of Science, under the auspices of the Biophysics Department.